Scattering of GeV electrons by nuclear matter

O. Benhar
Istituto Nazionale di Fisica Nucleare, Sezione Sanitá, I-00161 Roma, Italy

A. Fabrocini
Department of Physics, University of Pisa, I-56100 Pisa, Italy

S. Fantoni
International School for Advanced Studies, I-34014 Trieste, Italy

G. A. Miller
Department of Physics, University of Washington, Seattle, Washington 98195

V. R. Pandharipande
Department of Physics, University of Illinois, Urbana, Illinois 61801

I. Sick
Department of Physics, University of Basel, CH-4056, Basel, Switzerland
(Received 7 March 1991)

The cross section for inclusive electron scattering by nuclear matter is calculated at high momentum transfers using a microscopic spectral function, and compared with that extrapolated from data on laboratory nuclei. It is found that the cross section obtained with the plane-wave impulse approximation is close to the observed data at large values of the energy loss, but too small at low values. In this regime final-state interactions are important; after including their effects theory and data are in fair agreement. It is necessary to treat nucleon-nucleon correlations consistently in estimating the final-state interactions. The effects of possible time dependence of the nucleon-nucleon cross section, giving rise to nuclear transparency, are also investigated. The y scaling of the response function is discussed to further elucidate the role of final-state interactions.

I. INTRODUCTION

The many-body theory of nuclei [1,2], based on the assumption that nuclei can be treated as bound states of interacting nonrelativistic nucleons, has been successful [3] in explaining a number of nuclear properties. Scattering of 100–1000 MeV electrons, particularly by light nuclei, provides interesting tests for the nuclear many-body theory (NMBT). Many of the observables [4–9] could be understood. However, a number of problems, such as the lack of strength in the Coulomb sum of the longitudinal response or the behavior of the response at very low or high energy loss, remain to be fully resolved.

The scattering of multi-GeV electrons is expected to provide more stringent tests for the nuclear many-body theory. It can also be expected to give insights towards a deeper understanding of nuclei in terms of more fundamental degrees of freedom.

Of significant importance to this program are the recent experiments [10] in which inclusive scattering of multi-GeV electrons by different nuclear targets was studied. In particular, by examining the mass dependence of the scattering data, it has been possible [11] to extract the inclusive cross sections for nuclear matter. Among all nuclear systems, nuclear matter and few-body nuclei can be most accurately treated theoretically. In this paper, we attempt to understand the extrapolated nuclear matter inclusive cross section within the framework of NMBT.

There are two main problems in applying NMBT to scattering of multi-GeV electrons. For the momentum transfers of interest, after the scattering process, the struck nucleon has momenta of the order of the nucleon mass m, i.e., it is relativistic. Moreover, much of the response arises from the struck nucleon being promoted to an excited hadronic state.

The relativistic kinematics of the struck nucleon has a significant effect that can be easily seen in the response of a simple Fermi gas. In the nonrelativistic case the response is peaked at $|\mathbf{q}|^2/2m$ and has a width of the order $k_F|\mathbf{q}|/m$, where $\mathbf{q}$ is the momentum transfer and k_F is the Fermi momentum. In the extreme relativistic limit ($|\mathbf{q}| \gg m$), the response has a peak at $|\mathbf{q}|$ and a width of k_F. In the commonly used approximation discussed in this paper, final-state interactions (FSI) lead to a folding of the response. In the nonrelativistic case, the width of the response, due to the momentum distribution in the initial state, is proportional to $|\mathbf{q}|$, as it is in the case of strongly interacting quantum liquids. If the width of the folding function is finite, then it can be argued that, at large enough values of $|\mathbf{q}|$, FSI can be neglected, and, as a consequence, the response will exhibit y scaling. In contrast, in the case of the nuclear medium at high q, one has to use relativistic kinematics and therefore the width of the response due to the momentum distribution of particles in the initial state is roughly constant $\sim k_F$. It then follows that FSI effects can be neglected only if the folding width goes to zero at large q. The folding width is of the order of the imaginary part of the optical potential which is ~ 60 MeV $\sim k_F/4$ for several hundreds MeV nucleons. Therefore, FSI are not obviously negligible in scattering of multi-GeV electrons by nuclei.

Ideally, one should start from a realistic relativistically covariant theory of nuclei; however, such a theory is not yet practicable due to difficulties in treating pion-exchange interactions. In the plane-wave impulse approximation (PWIA), the FSI of the struck relativistic hadron is neglected. For a PWIA calculation of the response, one requires only the knowledge of the spectral function of the target ground state, which can presumably be calculated with the nonrelativistic NMBT, as the relativistic aspect concerns mainly the knocked-out nucleon. The calculation of the response within PWIA using relativistic dynamics for the struck hadron and the nonrelativistic spectral function is discussed in Sec. II. In this calculation, the off-shell electron-nucleon vertices are treated according to the approach of De Forest [12], generalized to include inelastic scattering on the nucleon. It is found that the PWIA cross section is close to the experimental one at values of ω corresponding to the quasi-free peak ($\omega_{qf}=\sqrt{|\mathbf{q}|^2+m^2}-m$) and beyond, but too small at lower values.

In Sec. III, an approach based on the multiple-scattering Glauber theory is used to take the FSI into account. We use the experimental N–N amplitude and include the effect of short-range correlations by using the calculated pair distribution function of nuclear matter. The possible relevance of the hadronization time of the struck nucleon is also investigated. The results are discussed in Sec. IV along with possible improvements in the theory. Finally, in Sec. V we discuss the y scaling of the response in order to further elucidate the role played by the FSI.

II. PWIA AND ELECTRON-NUCLEON VERTEX

The cross section for the inclusive reaction

$$e+A\rightarrow e'+\text{anything} \tag{2.1}$$

is given by [13]

$$\frac{d^2\sigma}{d\Omega\,d\epsilon'}=\frac{\alpha^2}{q^4}\frac{\epsilon'}{\epsilon}L^{\mu\nu}W^A_{\mu\nu}(q)\ , \tag{2.2}$$

where $\alpha=\frac{1}{137}$ is the fine-structure constant and $L^{\mu\nu}$ and $W^A_{\mu\nu}$ are the lepton and the nucleus tensors, respectively. The electron mass can be safely neglected in $L^{\mu\nu}$, which then can be written as

$$L^{\mu\nu}=2[k^\mu k'^\nu+k^\nu k'^\mu-g^{\mu\nu}(k\cdot k')]\ , \tag{2.3}$$

$k\equiv(\epsilon,\mathbf{k})$ and $k'\equiv(\epsilon',\mathbf{k}')$ being the four-momenta of the incident and the scattered electron, with $q\equiv(\omega,\mathbf{q})=k-k'$.

The explicit calculation of the nuclear tensor

$$W^A_{\mu\nu}(q)=\sum_N\int d\mathbf{p}_N\langle O|J^A_\mu|N\rangle \times\langle N|J^A_\nu|O\rangle\delta^{(4)}(p_0+q-p_N)\ , \tag{2.4}$$

at large momentum transfer ($|\mathbf{q}|>m$), requires a consistent relativistic description of both the initial and final nuclear states $|O\rangle$ and $|N\rangle$, as well as of the nuclear current J^A. Unfortunately, such a description is out of reach of the existing relativistic many-body approaches. However, it is believed that reasonable approximations to $W^A_{\mu\nu}$ can be obtained by starting from and improving upon PWIA.

The physical motivation for the PWIA comes from the fact that the electron probes a region of dimensions $\sim 1/|\mathbf{q}|$ of the nuclear target; therefore, for large enough momentum transfers, one can assume that the scattering process involves only one nucleon, the residual $(A-1)$-particle system acting as a spectator. This assumption leads to two drastic simplifications in the structure of $W^A_{\mu\nu}$: (i) the nuclear current operator can be written as the sum of the one-body nucleon currents; and (ii) the final nuclear state reduces to the product of a one-particle state, describing the free propagation of the struck nucleon, and an $(A-1)$-particle state of the spectator system. As a result, the dynamics of the nuclear target is decoupled from the electromagnetic vertex, and the relativistic description of the motion of the struck hadron reduces to a purely kinematical problem, which can therefore be treated exactly.

The PWIA expression of the target tensor is given by [12] (see Fig. 1 for the definitions of the kinematical variables)

$$W^A_{\mu\nu,\mathrm{IA}}(q)=\int d\mathbf{p}\,dE P(\mathbf{p},E)[Z\tilde{W}^p_{\mu\nu}(\mathbf{p},E,q) +N\tilde{W}^n_{\mu\nu}(\mathbf{p},E,q)]\ , \tag{2.5}$$

where the nucleon spectral function $P(\mathbf{p},E)$ represents the probability distribution for leaving the residual nu-

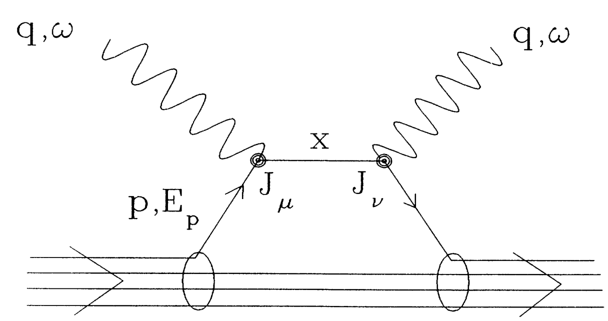

FIG. 1. PWIA scattering process.

cleon of momentum $\mathbf{p}$ from the target nucleus. The off-shell proton and neutron tensors $\tilde{W}^p_{\mu\nu}$ and $\tilde{W}^n_{\mu\nu}$ are related to the structure functions of the free nucleons, which are measured in elastic and inelastic electron-proton and electron-deuteron scattering experiments.

A. Nuclear matter spectral function

A calculation of $P(\mathbf{p},E)$ for infinite nuclear matter has been recently carried out [14] within the framework of correlated basis function (CBF) perturbation theory using a complete set of orthonormal correlated many-body wave functions (OCB states), generated by a realistic nuclear Hamiltonian, involving two-body and three-body interactions.

In Ref. [14], the following expression of the spectral function has been adopted:

$$P(\mathbf{p},E)=\sum_N |\langle N|a_{\mathbf{p}}|O\rangle|^2\delta(E-E_N+E_O) , \qquad (2.6)$$

where $|O\rangle$ represents the nuclear matter ground state, with energy eigenvalue E_O, whereas $|N\rangle$ and E_N, respectively, denote eigenstates and energies of the $(A-1)$-particle system. The energy E_N and E_O do not include nucleon rest mass. *One-hole–* and *two-hole–one-particle* intermediate OCB states have been included in the calculation.

The contribution from two-body breakup processes, corresponding to one-hole intermediate OCB states, turns out to be sharply peaked at $E=-e(\mathbf{p})$, $e(\mathbf{p})$ being the excitation energy of the one-hole OCB state of momentum $\mathbf{p}$, with $p<k_F$. The width of the peak provides a measure of the lifetime of the corresponding quasihole state and goes to zero as $|\mathbf{p}|$ approaches the Fermi momentum k_F. These two-body breakup processes dominate the PWIA dynamic structure function given by

$$S_{\mathrm{IA}}(\mathbf{q},\omega)=\int d\mathbf{p}\, dE P(\mathbf{p},E)\delta(\omega-E-e_0(|\mathbf{p}+\mathbf{q}|)) , \qquad (2.7)$$

with $e_0(\mathbf{p})=(|\mathbf{p}|^2+m^2)^{1/2}-m$, in the region of the quasifree peak. They have been studied in $(e,e'p)$ experiments for a variety of targets, ranging from the few-nucleon systems to heavy nuclei [15,16].

A completely different energy dependence is displayed by the contribution to $P(\mathbf{p},E)$ coming from three-body breakup processes, associated with two-hole–one-particle intermediate OCB states in Eq. (2.6). These processes, produced by nucleon-nucleon correlations, give rise to the appearance of a widespread *background*, extending up to large values of both $|\mathbf{p}|$ and E (see Fig. 2), and yield the dominant contribution to Eq. (2.7) in the kinematical regions corresponding to the tails of the quasifree peak.

The energy dependence of $P(\mathbf{p},E)$, which is typical of a strongly interacting Fermi fluid, has been shown [14] to play a crucial role in the determination of the PWIA response. Neglecting this dependence, which amounts to replacing the spectral function with the momentum distribution in the evaluation of the PWIA response, leads to a sizable overestimate of $S_{\mathrm{IA}}(\mathbf{q},\omega)$ in the low-ω region,

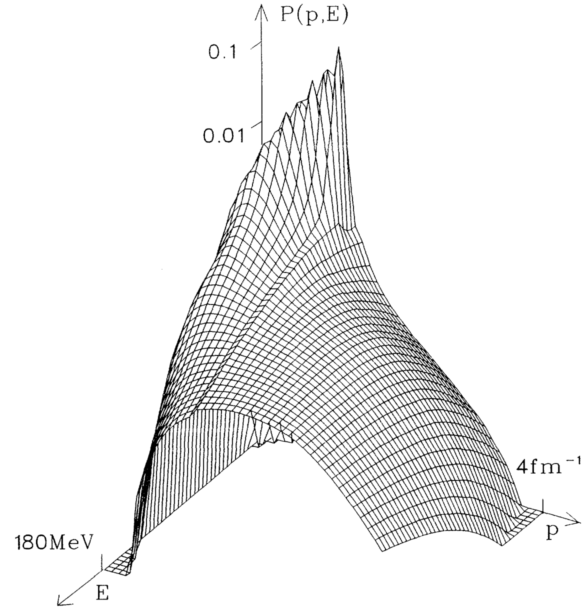

FIG. 2. Spectral function $P(p,E)$ of nuclear matter.

even at very high values of the momentum transfer $(|\mathbf{q}|\sim 1.5\ \mathrm{GeV}/c)$ [14,17].

B. Off-shell electron-nucleon cross section

The relevance of the high-momentum and high-energy components of the spectral function in the determination of the nuclear matter response implies that, in order to evaluate the cross section (2.2), the treatment of the electron-nucleon vertex for an off-shell nucleon has to be carefully considered.

Since the scattering process involves a bound particle, a fraction of the energy transferred by the virtual photon goes into excitation energy of the residual $(A-1)$-particle system, and the four-momentum transferred to the struck nucleon is given by [12] $\tilde{q}\equiv(\mathbf{q},\tilde{\omega})$, the off-shellness being measured by the quantity

$$\omega-\tilde{\omega}=E+(|\mathbf{p}|^2+m^2)^{1/2}-m . \qquad (2.8)$$

The spectral function $P(\mathbf{p},E)$ is zero for E less than 16 MeV, the binding energy per nucleon of nuclear matter. As a consequence, $\omega-\tilde{\omega}$ is greater than 16 MeV and, the larger $|\mathbf{p}|$ or E is, the more off shell the nucleon is.

In Ref. [12], deForest proposed to describe the elastic scattering of an electron by an off-shell nucleon using the free-nucleon spinors and current operators, but replacing the electron momentum transfer q with $\tilde{q}$. Moreover, imposing gauge invariance

$$q_\mu \tilde{W}^{\mu\nu}=\tilde{W}_{\mu\nu}q^\nu=0 , \qquad (2.9)$$

one can eliminate the dependence of the off-shell nucleon tensor upon the longitudinal current. The contribution to the cross section (2.2) due to elastic $e-N$ processes, is then given by [18]

$$\left[\frac{d^2\sigma}{d\Omega\, d\epsilon'}\right]_{\rm el} = \int d\mathbf{p}\, dE P(\mathbf{p},E) \times [Z\sigma_{ep}^{\rm el}(|\mathbf{q}|,\tilde{\omega}) + N\sigma_{en}^{\rm el}(|\mathbf{q}|,\tilde{\omega})] , \quad (2.10)$$

where the elastic $e-N$ ($N=p,n$) cross section is

$$\sigma_{eN}^{\rm el} = \sigma_M \frac{m}{E_p}\left[T_1 W_1^N(\tilde{q},\tilde{q}\cdot p) + T_2 \frac{W_2^N(\tilde{q},\tilde{q}\cdot p)}{m^2}\right] \quad (2.11)$$

with

$$T_1 = 2\tan^2\frac{\theta}{2} + \frac{q^2}{|\mathbf{q}|^2}\left[\frac{q^2}{\tilde{q}^2} - 1\right] , \quad (2.12)$$

$$T_2 = (|\mathbf{p}|^2 - p_\parallel^2)\left[\tan^2\frac{\theta}{2} - \frac{1}{2}\frac{q^2}{|\mathbf{q}|^2}\right] + \frac{q^4}{|\mathbf{q}|^4}\frac{(E_p + E_{p'})^2}{4} . \quad (2.13)$$

In the above equation σ_M denotes the Mott cross section, $E_p = (|\mathbf{p}|^2 + m^2)^{1/2}$, $E_{p'} = (|\mathbf{p}+\mathbf{q}|^2 + m^2)^{1/2}$, $\tilde{q}\cdot p = \tilde{\omega}E_p - \mathbf{q}\cdot\mathbf{p}$, and $p_\parallel$ is the component of $\mathbf{p}$ parallel to the momentum transfer $\mathbf{q}$. The elastic nucleon structure functions W_1^N and W_2^N are expressed in terms of the usual electric and magnetic form factors G_E^N and G_M^N by the following relations:

$$W_1^N(\tilde{q},\tilde{q}\cdot p) = -\frac{\tilde{q}^2}{2m}[G_M^N(q^2)]^2 \delta(s - m^2) , \quad (2.14)$$

$$W_2^N(\tilde{q},\tilde{q}\cdot p) = \frac{2m}{(1 - q^2/4m^2)}\left[[G_E^N(q^2)]^2 - \frac{q^2}{4m^2}[G_M^N(q^2)]^2\right] \times \delta(s - m^2) , \quad (2.15)$$

$s = (p + \tilde{q})^2$ being the squared invariant mass of the final state of the struck nucleon.

The de Forest approach is readily generalized to describe not only elastic but also inelastic electron scattering by an off-shell nucleon. In fact, the inelastic cross section $\sigma_{eN}^{\rm inel}$ has the same expression as in Eq. (2.11) with $W_1^N(\tilde{q},\tilde{q}\cdot p)$ and $W_2^N(\tilde{q},\tilde{q}\cdot p)$, given in Eqs. (2.14) and (2.15), replaced by the corresponding inelastic structure functions $W_{1,in}^N(\tilde{q},\tilde{q}\cdot p)$ and $W_{2,in}^N(\tilde{q},\tilde{q}\cdot p)$. They are parametrized to fit the data and are given in Ref. [19] as a product of two functions, describing the threshold and resonance region and the deep inelastic region, respectively. The inelastic contribution $(d^2\sigma/d\Omega\, dE')_{\rm inel}$ is then obtained from Eq. (2.10), when the $\sigma_{eN}^{\rm el}$ are substituted with $\sigma_{eN}^{\rm inel}$.

Figure 3 shows the calculated PWIA cross sections for incident electron energy $\epsilon = 3.595$ GeV and scattering angle $\theta = 30°$, compared with the *nuclear matter data* and deserves the following comments.

For the kinematical conditions of Fig. 3, corresponding to momentum transfers $|\mathbf{q}| \sim 2$ GeV/c, the inelastic contribution turns out to be comparable with that due to elastic e-N scattering already in the region of the quasifree peak ($\omega \sim 1.2$ GeV) and becomes dominant at $\omega \sim 1.5$ GeV.

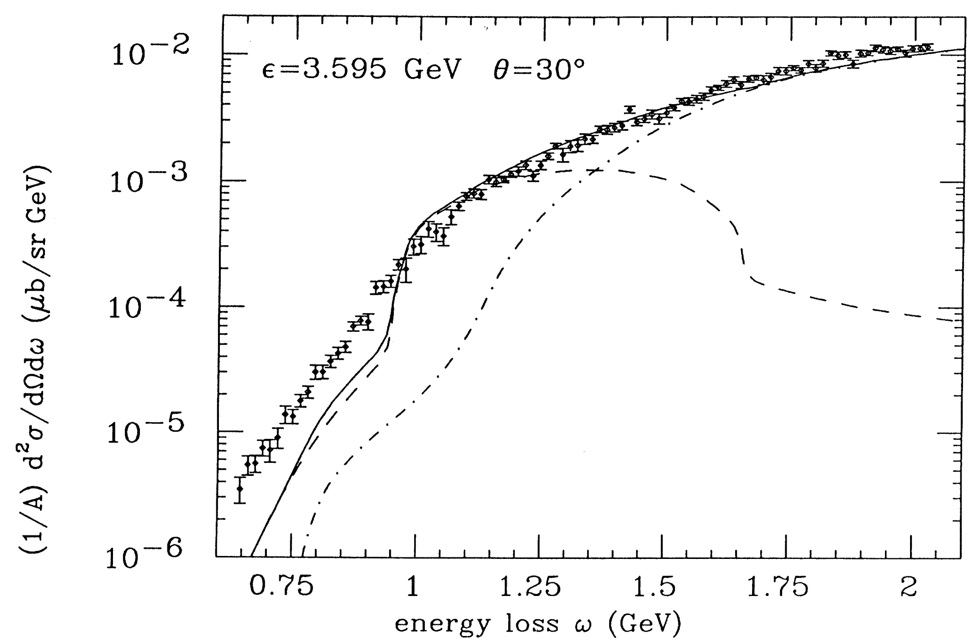

FIG. 3. PWIA inclusive cross section for incident electron energy $\epsilon = 3.595$ GeV and scattering angle $\theta = 30°$, compared with the experimental data of Ref. [11]. The dashed and the dot-dashed lines give the contributions from the elastic and the inelastic e-N scattering processes, respectively.

The calculation of the inelastic contribution carried out in the present work, which consists in using the full nuclear matter spectral function $P(p,E)$ and in describing the off-shell nucleon tensor according to deForest's prescription, has to be regarded as a significant improvement upon the estimate of Ref. [11]. Such an estimate was, in fact, based on the procedure originally proposed by Bodek and Ritchie [19]. According to this procedure, the dependence upon the excitation energy of the residual system is disregarded both in the spectral function, which is approximated by the momentum distribution, and in the off-shell extrapolation of the nucleon tensor. The momentum distribution used in Ref. [11] has been extracted by the y-scaling analysis of the data. The inclusion of the dependence upon E and the treatment of the nucleon off-shellness according to de Forest's prescription play a relevant role in determining the inelastic cross section. In the resonance and threshold region, the use of $\tilde{q}$ instead of q leads to a sizable change in the values of the inelastic structure functions. For instance, at $\epsilon=3.995$ GeV, $\theta=30°$ and $\omega \sim 1.35$ GeV, we get a value of $\sim 0.76\times 10^{-4}$ μb/sr GeV for the inelastic contribution to the cross section, which is to be compared to the estimate of $\sim 1.5\times 10^{-4}$ μb/sr GeV reported in Ref. [11].

The results from the present calculation and the data are in close agreement at $\omega > 1$ GeV, whereas sizable discrepancies occur, in both magnitude and shape, at lower energy loss. It appears that the theoretical curve lies a factor of 3–4 below the data at $\omega=0.7$–0.8 GeV, and exhibits a pronounced kink at $\omega \sim 0.9$ GeV, reflecting the threshold for the three-body breakup processes. The origin of this kink can be traced back to the discontinuity of the nuclear matter momentum distribution at $p=k_F$.

III. EFFECTS OF FINAL-STATE INTERACTIONS

In order to estimate the effects of the FSI on the nuclear tensor $W^A_{\mu\nu}(q,\omega)$, it is convenient to use the following expression:

$$W^A_{\mu\nu}(q,\omega)=2\Re\int_0^\infty dt\,\langle O|J^A_\mu(q)e^{-i(H-E_0-\omega)t}J^A_\nu(q)|O\rangle\ , \tag{3.1}$$

which is equivalent to Eq. (2.4). From now on, the quantity q will denote the modulus of the three-momentum transfer $\mathbf{q}$, namely, $q\equiv|\mathbf{q}|$. The effects of the interactions between the particles of the target, in both the initial and the final states, can be consistently treated with this equation. In fact, it has been used with CBF theory to calculate the nonrelativistic response of nuclear matter [20,21,14] and liquid helium [22,23].

As explained in Sec. II, approximate treatments based upon PWIA are obtained by assuming that, at large enough momentum transfers, the contributions due to the exchange of the struck hadron with other nucleons is negligible, and thus the struck nucleon can be considered as a distinct particle. In this case one can consider the Hamiltonian H as given by

$$H=H_0+H_I\ , \tag{3.2}$$

where the *unperturbed* Hamiltonian H_0 contains the sum of the free Hamiltonian of the struck hadron and the Hamiltonian of the remaining $A-1$ nucleons in the target nucleus including their interactions. The *interaction* Hamiltonian H_I contains only the FSI of the struck nucleon with the other $A-1$ nucleons.

Let $|N\rangle$ be an eigenstate of the $A-1$ nucleons, $|X\rangle$ be the state of the struck hadron, and

$$(H_0-E_0)|N\rangle|X\rangle=\omega_{NX}|N\rangle|X\rangle\ , \tag{3.3}$$

where E_0 is the ground-state energy of the nucleus. The PWIA is obtained by neglecting H_I, so that

$$\begin{aligned}W^A_{\mu\nu,IA}(q,\omega)&=2\Re\int_0^\infty dt\,\langle O|J^A_\mu(q,\omega)e^{-i(H_0-E_0-\omega)t}J^A_\nu(q,\omega)|O\rangle\\&=\sum_{N,X}\delta(\omega-\omega_{NX})\langle O|J^A_\mu(q,\omega)|N\rangle|X\rangle\langle X|\langle N|J^A_\nu(q,\omega)|O\rangle\ ,\end{aligned} \tag{3.4}$$

as calculated in the last section.

In Ref. [24], Horikawa et al. originally proposed to describe the FSI in terms of an optical potential. It is easy to verify that if the effect of H_I is represented by means of an *optical potential* $V-iW$ defined such that

$$\begin{aligned}&\langle O|J^A_\mu(q,\omega)e^{-i(H-E_0-\omega)t}J^A_\nu(q,\omega)|O\rangle\\&\quad\equiv e^{-i(V-iW)t}\langle O|J^A_\mu(q,\omega)e^{-i(H_0-E_0-\omega)t}J^A_\nu(q,\omega)|O\rangle\ ,\end{aligned} \tag{3.5}$$

then the V and the W must depend upon q, ω, and t. In fact, inverting Eq. (3.1), one gets the relation

$$\langle O|J^A_\mu(q,\omega)e^{-i(H-E_0)t}J^A_\nu(q,\omega)|O\rangle=\frac{1}{2\pi}\int_{-\infty}^{\infty}d\omega\,W^A_{uv}(q,\omega)e^{-i\omega t}\ , \tag{3.6}$$

and a similar relation is obtained from Eq. (3.4) with H_0 and $W^A_{\mu\nu,\mathrm{IA}}(q,\omega)$ in place of H and $W^A_{\mu\nu}(q,\omega)$, respectively. Therefore, Eq. (3.5) implies that

$$\int d\omega\,W^A_{\mu\nu}(q,\omega)e^{-i\omega t}=\int d\omega\,W^A_{\mu\nu,\mathrm{IA}}(q,\omega)e^{-i(V-iW)t}e^{-i\omega t}\ . \tag{3.7}$$

In practice, one uses approximations for V and W. Note that the imaginary potential $W(q,\omega,t)$ has to be defined such that $W(q,\omega,-t)=-W(q,\omega,t)$ so that $\exp[-W(q,\omega,t)]<1$ for both $t>0$ and $t<0$. The following simple convolution formulas are obtained if $V(q)$ is assumed to be independent of ω and t and $W(q,t)$ independent of ω:

TABLE I. Quasifree kinematics and parameters of the N-N amplitude.

ϵ (GeV)	θ (deg)	ϵ' (GeV)	$\omega_{\rm qf}$ (GeV)	q (fm^{-1})	v/c	β (fm)	σ_{NN} (mb)
3.595	20	2.921	0.674	6.65	0.813	0.20	35.0
3.595	25	2.646	0.949	8.30	0.868	0.25	40.0
3.595	30	2.376	01.219	9.85	0.900	0.29	43.3
3.995	30	2.545	01.450	11.13	0.920	0.32	43.3

$$W^A_{\mu\nu}(q,\omega)=\int_0^\infty d\omega' F(\omega-\omega')W^A_{\mu\nu,\rm IA}(q,\omega'-V(q)) , \tag{3.8}$$

$$F(\omega-\omega')=\frac{1}{\pi}\Re\int_0^\infty dt\, e^{i(\omega-\omega')t}e^{-W(q,t)t} . \tag{3.9}$$

They have been used to estimate the effect of the FSI in deep-inelastic scattering of neutrons by liquid helium [25–28].

The simplest approximation for V and W is to use the real and imaginary parts of the optical potential of the hadron X in nuclear matter. The effects of the FSI are very important only at small values of ω where the response is dominated by elastic $e-N$ processes in which X is a *nucleon* having momentum ~ 2 GeV/c (Fig. 3). Dirac optical modes fits [29,30] to the scattering of 0.1–1 GeV protons by nuclei suggest that $V\sim 25$ MeV in the region of interest, and it has a rather small effect on the response. Thus, the main effect of the FSI is due to the damping of the motion of the struck nucleon described by the imaginary potential W.

The crudest estimate for W is obtained by taking the time-independent

$$W(p')=\frac{\hbar}{2}\rho v(p')\sigma_{NN}(p') , \tag{3.10}$$

where ρ is the density (0.16 fm^{-3}) of nuclear matter, $v(p')$ and $\sigma_{NN}(p')$ are, respectively, the velocity and the scattering cross section of the struck nucleon. In fact, the momenta p' of the struck nucleon have a spread in magnitude of $\sim k_F$ around the average value q. However, in the region of interest here, v is close to c and σ_{NN} does not depend strongly on p' (see Table I). Hence, it is reasonable to calculate both v and σ_{NN} for nucleons having momentum q.

The time-independent W gives a Lorentzian folding function

$$F_L(\omega-\omega')=\frac{W}{\pi}\left[\frac{1}{W^2+(\omega-\omega')^2}\right] , \tag{3.11}$$

which has unrealistically long tails (see Fig. 4). In nonrelativistic quantum liquids, the use of a Lorentzian folding function violates the ω^2 sum rule. In the present case it gives too large response at small values of ω (see Fig. 5). It is believed that the major source of inaccuracies in $F_L(\omega-\omega')$ comes from neglecting the fact that the struck nucleon was a part of the ground state [25]. The particles surrounding the struck nucleon are not uniformly distributed at density ρ, rather the density $\rho(r)$ of nucleons at a distance r from a nucleon in the ground state is given by $\rho g(r)$, where $g(r)$ is the pair distribution function [31] shown in Fig. 6. At small r, $g(r)$ becomes very small and, consequently, the motion of the struck nucleon is essentially undamped at small value of the time t.

Multiple-scattering Glauber theory [32,33] provides a framework for obtaining approximate expressions for $W(q,t)$ which take into account the ground-state correlations. The struck nucleon is assumed to be at $r=0$ and $t=0$ when it is struck. Its wave function at $t>0$ is written as

$$\Psi^{(+)}(q,z)=e^{iqz}\Phi(z) , \tag{3.12}$$

where $z=\mathbf{r}\cdot\hat{\mathbf{q}}$ and $\Phi(z)$ is defined as

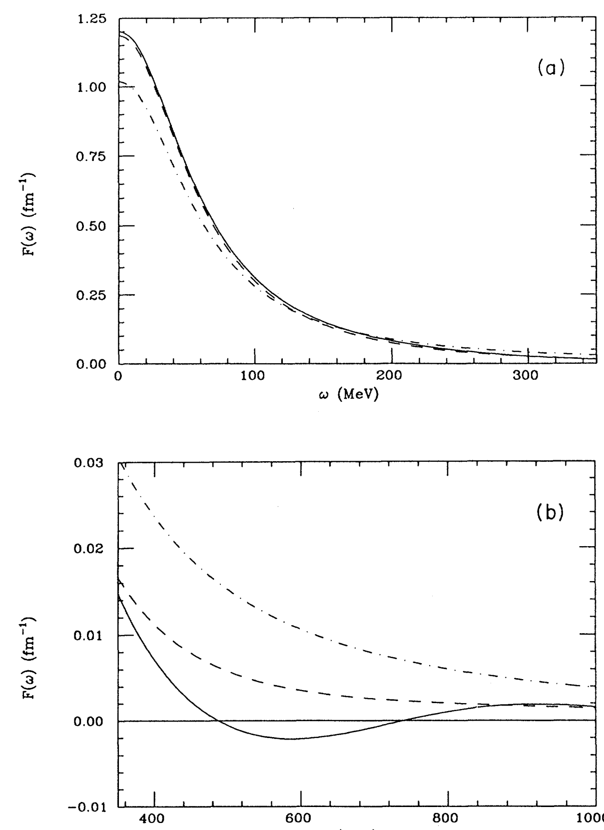

FIG. 4. Low and high ω behaviors of the folding functions used in the calculation of the FSI at E=3.595 GeV, θ=30°. The dot-dashed, dashed, and solid lines denote the Lorentzian F_L, the correlated Glauber F_G, and the correlated Glauber plus color transparency $F_{\rm GCT}$ folding functions, respectively.

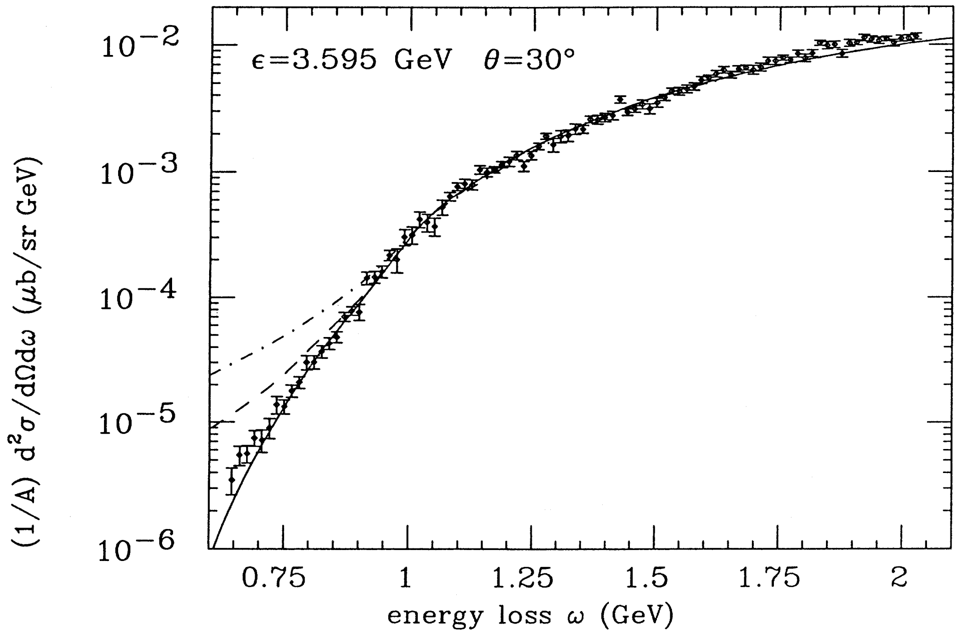

FIG. 5. Calculated cross section for incident electron energy $\epsilon=3.595$ GeV and scattering angle $\theta=30°$, compared with the experimental data. The dot-dashed and the dashed lines correspond to the results obtained with F_L and F_G, respectively. The solid line is obtained with $F_{\rm GCT}$.

$$\Phi[z=v(q)t]\equiv\exp\left[-i(V-iW)\frac{z}{\hbar v(q)}\right] . \quad (3.13)$$

The eikonal approximation,

$$\Phi(z)=\exp\left[\frac{-i}{\hbar v(q)}\int_0^z d\xi\, v_{\rm int}(\xi)\right] , \quad (3.14)$$

is used to calculate $\Phi(z)$ and the q and t dependent optical potential V and W in Eq. (3.13). This approximation is valid if the quantity $v_{\rm int}\Phi$ varies slowly within distances of the order of $1/q$ and if $v_{\rm int}/E_q \ll 1$. The $v_{\rm int}(\xi)$ represents the interaction of all the nucleons with the struck nucleon and it is taken as

$$v_{\rm int}=\sum_i v_{{\rm eff},q}(\mathbf{r}-\mathbf{r}_i) , \quad (3.15)$$

where $\mathbf{r}_i$ denotes the positions of the other nucleons. The $v_{{\rm eff},q}$ is obtained from the free N-N scattering data as

$$v_{{\rm eff},q}(\mathbf{r})=-\frac{2\pi\hbar}{m}\int\frac{d\mathbf{k}}{(2\pi)^3}e^{i\mathbf{k}\cdot\mathbf{r}}f_q(\mathbf{k}) , \quad (3.16)$$

where $f_q(\mathbf{k})$ is the amplitude for the scattering of a nucleon of momentum q, with momentum transfer $\mathbf{k}$, by free nucleons at rest.

If the ground-state correlations are neglected, Eq. (3.15) becomes

$$v_{\rm int}(\mathbf{r})=-\frac{2\pi\rho\hbar^2}{m}\int\frac{d\mathbf{k}}{(2\pi)^3}d\mathbf{r}'e^{i\mathbf{k}\cdot(\mathbf{r}-\mathbf{r}')}f_q(\mathbf{k})$$
$$=-\frac{2\pi\rho\hbar^2}{m}f_q(k=0) . \quad (3.17)$$

Substituting this $v_{\rm int}(\mathbf{r})$ in Eq. (3.14), we get the trivial result

$$W(q)=\frac{2\pi\rho\hbar^2}{m}\Im(f_q(k=0))$$
$$=\frac{\hbar}{2}\rho v(q)\sigma_{NN}(q) . \quad (3.18)$$

In order to include the effects of the correlations among the hole associated with the struck nucleon and the remaining nucleons, in first-order approximation, $v_{\rm int}(\mathbf{r})$ is given by

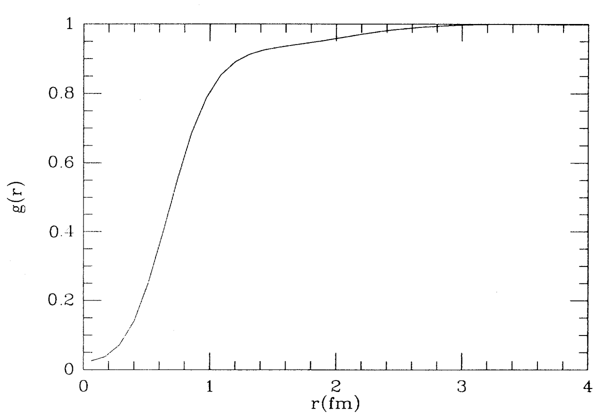

FIG. 6. Pair distribution function of nuclear matter at the empirical saturation density ($k_F=1.33$ fm^{-1}).

$$v_{\rm int}(\mathbf{r})=\rho\int d\mathbf{r}' g(r')v_{{\rm eff},q}(\mathbf{r}-\mathbf{r}')\ , \tag{3.19}$$

and obtain

$$V-iW=-\frac{2\pi\rho v(q)}{q}\frac{1}{z}\int_0^z d\xi\int\frac{d\mathbf{k}}{(2\pi)^3}d\mathbf{r}'e^{i\mathbf{k}\cdot(\mathbf{r}'-\hat{\mathbf{q}}\xi)}g(r')f_q(\mathbf{k})\ . \tag{3.20}$$

A realistic parametrization of the imaginary part of the amplitude $f_q(\mathbf{k})$ is given by Bassel and Wilkin [34]:

$$If_q(\mathbf{k})=\frac{q}{4\pi}\sigma_{NN}e^{-[\beta(q)k]^2}\ . \tag{3.21}$$

The values of $\sigma_{NN}(q)$ and $\beta(q)$ have been tabulated by Dobrovolsky *et al.* [35] and by Silverman *et al.* [36] and interpolated in Table I for the kinematics of interest. We obtain

$$W(q,z)=\frac{\hbar}{2}\rho v(q)\sigma_{NN}(q)\left[1-\frac{1}{z}\int_0^z d\xi\int\frac{d\mathbf{k}}{(2\pi)^3}e^{-i\mathbf{k}\cdot\hat{\mathbf{q}}\xi}\frac{1-S(k)}{\rho}e^{-[\beta(q)k]^2}\right]\ , \tag{3.22}$$

where $S(k)$ is the static structure function:

$$S(k)=1+\rho\int d\mathbf{r}\,e^{i\mathbf{k}\cdot\mathbf{r}}[g(r)-1]\ . \tag{3.23}$$

The time-dependent $W(q,t)$ is identified as

$$W(q,t)=W(q,z=v(q)t)\ , \tag{3.24}$$

and the folding function [Eq. (3.9)] obtained with it is denoted by $F_{G}(\omega-\omega')$. It has no Lorentzian tail, as can be seen in Fig. 4, and gives a much improved description of the response (Fig. 5).

We now discuss some further approximations one could make in order to establish contact with other calculations. Since $\beta(q)$ in Eq. (3.22) is essentially the radius of the absorptive part of the N-N interaction and $1-S(k)$ becomes small at $kr_0\gg 1$, where r_0 is the unit radius ($4\pi r_0^3\rho/3=1$), $\beta(q)/r_0\ll 1$, and $\exp(-[\beta(q)k]^2)$ can then be approximated by unity to obtain

$$W(q,z)=\frac{\hbar}{2}\rho v(q)\sigma_{NN}(q)\frac{1}{z}\int_0^z d\xi\,g(\xi)\ , \tag{3.25}$$

or, equivalently,

$$W(q,t)=\frac{\hbar}{2}\rho v(q)\sigma_{NN}(q)\frac{1}{t}\int_0^t dt' g(v(q)t')\ . \tag{3.26}$$

The decay of the amplitude of the struck particle wave function,

$$\frac{d}{dt}(e^{-W(q,t)t})=-\frac{\hbar}{2}\rho v(q)\sigma_{NN}(q)g(v(q)t)e^{-W(q,t)t}\ , \tag{3.27}$$

seems to be governed by the density $\rho g(v(q)t)$ at time t.

The expression (3.22) derived within correlated Glauber theory has also been obtained from hard-core perturbation theory (HCPT), developed [28] for deep-inelastic neutron scattering on quantum fluids and solids, the only difference being the use of the t matrix in place of the experimental amplitude $-(4\pi\hbar^2/m)f_q$. In fact, by solving for $W(q,z)$ using the small-angle–large-l approximation for Legendre polynomials, Silver obtains [28], in the asymptotic limit,

$$W(q,t)=\frac{\hbar\rho v(q)\sigma_{NN}(q)}{2tr_c^2}\times\int_0^t dt'\int_0^{r_c}db\,b\,g(\sqrt{[v(q)t']^2+b^2})\ , \tag{3.28}$$

which reduces to Eq. (3.26) by assuming that r_c, the radius of the absorptive part of the $N-N$ interaction, is small.

The free $\sigma_{NN}(q)$ is used in the present work. There are several corrections to the $\sigma_{NN}(q)$ in matter. These can be grouped in three classes. In the first class we include those coming from the nucleonic degrees of freedom. These contain effects of multiparticle correlations, effective masses of nucleons in matter, screening effects, Pauli blocking effects, the ω dependence of σ_{NN}, etc. They are included in the nonrelativistic calculation [21] of the response of nuclear matter using CBF theory. These corrections are certainly important at low energies, however, they are expected to become less important at higher energies. Modifications of the $N-N$ amplitude at off-shell energies also play a role as shown by Uchiyama, Dieperink, and Scholten [37]; we neglect this here due to the lack of knowledge of the off-shell amplitude.

In the second class we may consider corrections to σ_{NN} due to changes in meson propagators in nuclear matter. These can equivalently be regarded as corrections due to three-body forces. Realistic models of three-body forces, obtained by fitting ground-state properties of light nuclei and nuclear matter [38] suggest that they are much weaker than the two-nucleon force and hence their effect on the folding function representing the FSI should be small. We expect that the main effects are already included by $g(r)$ which has indeed been calculated with the three-body force in the Hamiltonian.

The third class, finally, contains corrections to σ_{NN} due to the quark structure of the nucleons. The folding function $F(\omega-\omega')$ is sensitive to the interactions of the struck nucleon taking place within a fraction of 1 fm of its interaction with the electron, as demonstrated by the fact that it extends up to $\sim$700 MeV (see Fig. 4). It is then possible that these interactions differ significantly from the free $N-N$ interactions. Such an effect is generally discussed in the context of the phenomenon called *color transparency* [39–42], and we follow its treatment as given in the review by Frankfurt and Strickman [43]. In the parton model, the elastic $e-N$ scattering at large q could occur via the following process. The large-q virtual photon is absorbed when the quarks in the nucleon are in a compact *pointlike* configuration. This configuration can be regarded as a coherent superposition of different states of the baryon and evolves into a nucleon, i.e., the superposition gets out of phase in a time called the *hadronization length*

$$l_h = 2E_q/\Delta M^2 \ . \tag{3.29}$$

Various estimates of ΔM^2 can be found in the literature and we have used $\Delta M^2 = 0.7$ GeV^2 in the present work, as suggested by Ref. 41. The struck nucleon interacts with the other nucleons with the free σ_{NN} only after travelling a distance l_h. At $l < l_h$, the interaction cross section depends upon z and is estimated to be

$$\sigma(z<l_h) = \sigma_{NN}\left[\frac{z}{l_h}\left[1-\frac{9\langle k_T^2\rangle}{q^2-\omega^2}\right]+\frac{9\langle k_T^2\rangle}{q^2-\omega^2}\right] , \tag{3.30}$$

where k_T is the transverse momentum of partons in the nucleon ($\langle k_T^2\rangle^{1/2} \sim 350$ MeV). It is trivial to include such a time dependence of the cross section in the classical ($z = vt$) limit. We obtain

$$W_{\mathrm{GCT}}(q,z) = \frac{\hbar}{2}\rho v(q)\sigma_{NN}(q)\frac{1}{z}\int_0^z d\xi\, C(q,\xi)\left[1-\int\frac{d\mathbf{k}}{2\pi^3}e^{-i\mathbf{k}\cdot\hat{\mathbf{q}}\xi}\frac{1-S(k)}{\rho}e^{-[\beta(q)k]^2}\right] , \tag{3.31}$$

where

$$C(q,z) = 1+\Theta(l_h-z)\left[\frac{z}{l_h}-1\right]\left[1-\frac{9\langle k_T^2\rangle}{q^2-\omega^2}\right] , \tag{3.32}$$

and the resulting folding function denoted as F_{GCT} is also shown in Fig. 4. It has slightly smaller width than F_G, and the response obtained with it (see Fig. 5) is in better agreement with the data.

IV. RESULTS

The nuclear matter calculations are based on the following nonrelativistic Hamiltonian:

$$H = \sum_{i=1,A} -\frac{\hbar^2}{2m}\nabla_i^2 + \sum_{i<j=1,A} + \sum_{i<j<k=1,A} V_{ijk} , \tag{4.1}$$

where the Urbana two-body potential v_{ij} [44] and the three-nucleon interaction of Ref. [45] has been adopted to calculate the equation of state of nuclear matter. The evaluation of the spectral functions has been carried out within CBF theory (for a review see Ref. [46]). The correlated basis functions have been taken to be of the form

$$|n\rangle = \frac{G|n]}{[n|G^\dagger G|n]^{1/2}} , \tag{4.2}$$

where

$$G = S\prod_{j>i=1,A} F(i,j) , \tag{4.3}$$

$$F(i,j) = \sum_n f^n(r_{ij})O^n(i,j) , \tag{4.4}$$

with S being the symmetrization operator and the operators $O^n(i,j)$ include the four central components $[1;\sigma_i\cdot\sigma_j;\tau_i\cdot\tau_j;(\sigma_i\cdot\sigma_j)(\tau_i\cdot\tau_j)]$ for $N=1,4$ and the tensor components S_{ij} and $S_{ij}\tau_i\cdot\tau_j$ for $n=5,6$. The states $|n]$ are eigenfunctions of the Fermi gas Hamiltonian. The Löwdin-Schmidt orthogonalization procedure (LSOP) of Ref. [47] has been applied to orthogonalize the above complete set of basis functions $|n)$ to obtain the orthonormal set $|n\rangle$ used in the calculations. The details of the calculation of $P(\mathbf{p},E)$ are given in Ref. [14] and will not be reported here for brevity.

The single-particle excitation energies $e(k)$, appearing in Eq. (2.7), have been taken from the nonrelativistic calculation of Ref. [48], up to $k = k_L = 3.5$ fm^{-1}, and for $k > k_L$ from the relativistic expression

$$m + e(k) = \sqrt{(m+V_s)^2+k^2} + V_0 , \tag{4.5}$$

where the Lorentz vector and scalar potentials V_0 and V_s have been taken from volume term of the fit called case 1 by Cooper *et al.* [49] to ^{40}Ca elastic-scattering data [50,51] using phenomenological Dirac optical model. The real part of the nuclear matter optical potential U_{NM}

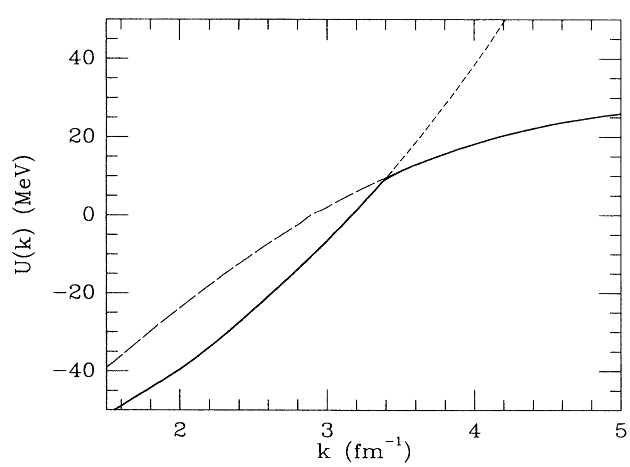

FIG. 7. Real part of the optical potential used in the calculation (solid line). The dashed and long-dashed curves represent the nonrelativistic and the relativistic calculations.

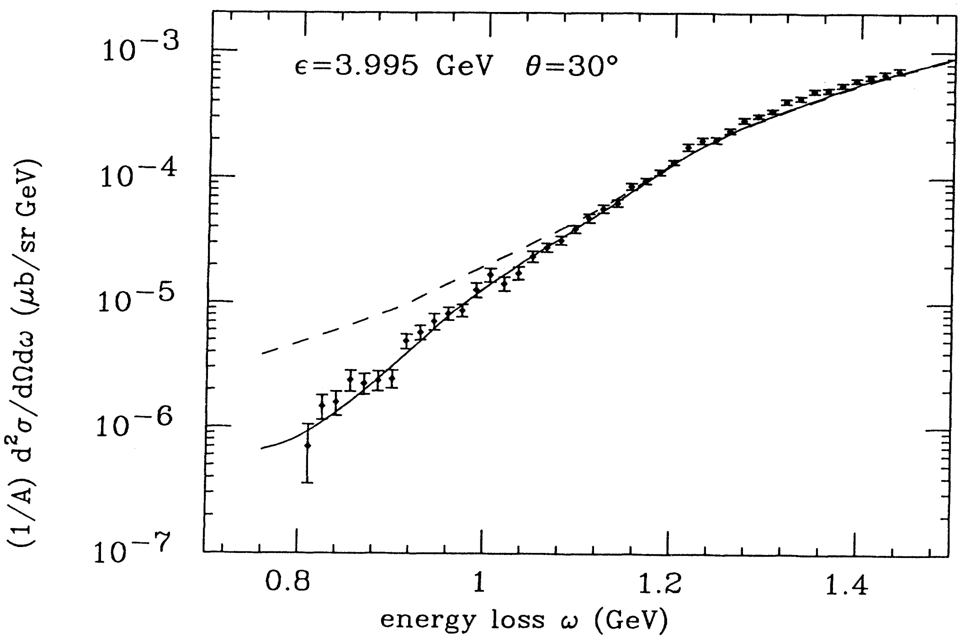

FIG. 8. Correlated Glauber (dashes) and correlated Glauber plus color transparency (solid line) results for the inclusive cross section at $\epsilon = 3.995$ GeV and scattering angle $\theta = 30°$.

is then extracted from the single-particle energies using the relation

$$m + e(k) = \sqrt{m^2 + k^2} + U_{\rm NM} \ . \tag{4.6}$$

The nonrelativistic and the relativistic U's cross at $k = k_L$ and are not very different in a broad region around k_L. At higher values of the momenta, the relativistic potential is roughly constant and ~25MeV, whereas the nonrelativistic one grows very rapidly (see Fig. 7). As mentioned earlier, the $U(k)$ is rather small in the region of interest, and therefore it has little effect on the calculated response.

The Höhler parametrization [52] of the free nucleon form factors has been employed in the calculation of the quasielastic cross section.

The results obtained for $\epsilon = 3.995$ GeV, $\theta = 30°$ are shown in Fig. 8 and for $\epsilon = 3.595$ GeV, $\theta = 25°$ and 20° are shown in Figs. 9 and 10. The theory is in good agree-

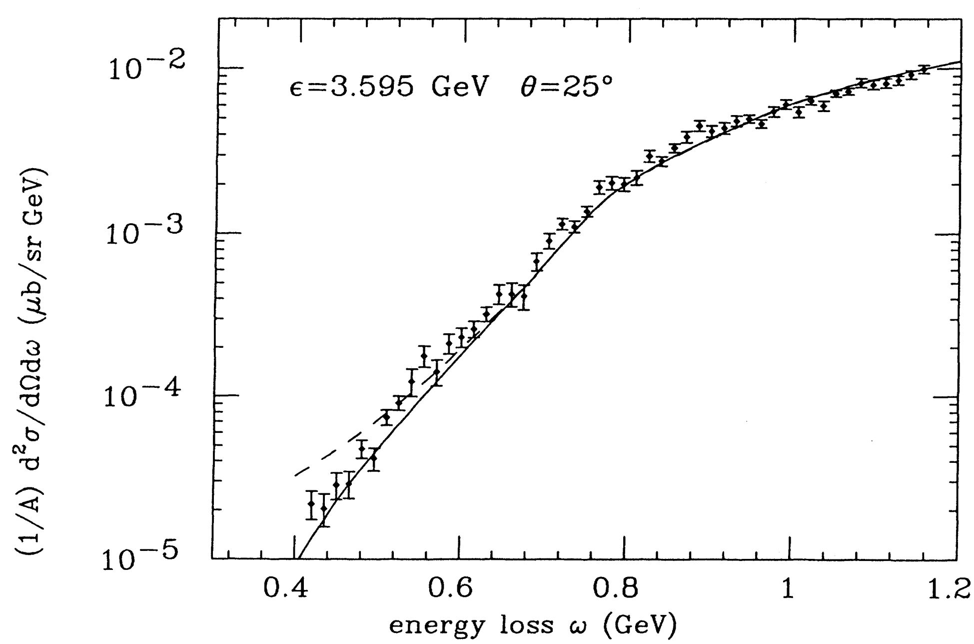

FIG. 9. As in Fig. 8 for $\epsilon = 3.595$ GeV and scattering angle $\theta = 25°$.

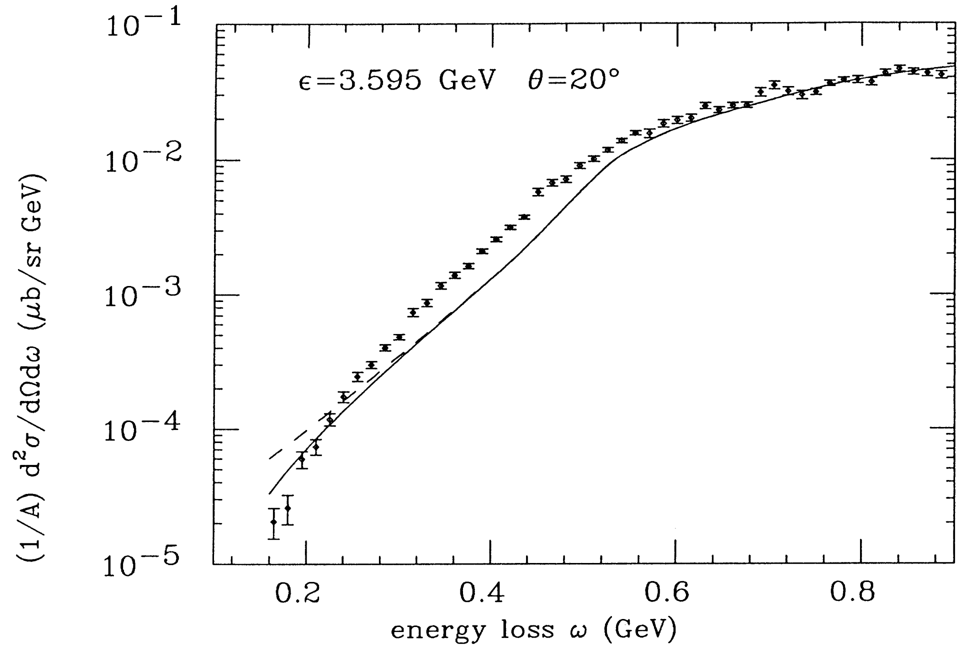

FIG. 10. As in Fig. 8 for $\epsilon = 3.595$ GeV and scattering angle $\theta = 20°$.

ment with the data at these values of E and θ. The PWIA response is too small at small ω, the estimated FSI is sufficient to raise the response up to the observed data. Particularly, at $\epsilon = 3.995$ GeV, $\theta = 30°$ the color transparency has a large effect on the response and it appears to be necessary in order to obtain agreement with the data. At very small ω the calculated cross sections at some kinematics have a flat behavior, which may be an artifact of the particular analytical structure of $\sigma(z)$ of Eq. (3.30). There is also some sensitivity to the high-energy behavior of the folding function. A natural cutoff is provided by the step size of the grid used in the tabulation of the distribution function $g(r)$. In our calculation such a cutoff lies in the region of 0.9 GeV which is the limiting value we have used for a nonvanishing $F(\omega)$.

V. SCALING

It is instructive to study the nuclear matter response not only in terms of the cross section, but also in terms of the scaling function $F(y)$. The quasielastic, inclusive response *a priori* is a function of two independent variables, q and ω. In the PWIA it can be shown that, as q tends to infinity, the cross sections will scale, i.e., become a function of a single variable y, this y being itself a function of q and ω. The variable y may be thought of as the minimal value of the momentum $\mathbf{p}$ of a nucleon bound with the minimal removal energy [53], allowed for by the energy- and momentum-conserving δ function

$$\delta(\sqrt{m^2+(\mathbf{p}+\mathbf{q})^2}-m+E-\omega)\ , \tag{5.1}$$

where E is the removal energy. In nuclear matter the minimal removal energy $E_{\min}$, given by the difference of the binding energies between the $A-1$ and the A systems, results to be 16 MeV. The minimal value of $\mathbf{p}$ occurs if $\mathbf{p}$ is (anti)parallel to $\mathbf{q}$, i.e., $y = p_{\parallel}$. The scaling function $F(y)$ is given by

$$F(y)=\frac{d\sigma}{d\Omega}(q,\omega)K^{-1}\tilde{\sigma}^{-1}\ , \tag{5.2}$$

where K is the kinematical factor, given by

$$K=\left|\frac{\partial\omega}{\partial p_{\parallel}}\right|^{-1}_{p=p_{\min}(E_{\min})}=\frac{\sqrt{m^2+(y+q)^2}}{q}\ , \tag{5.3}$$

and $\tilde{\sigma}$ is the sum of electron-proton and electron-neutron cross sections evaluated at an initial nucleon momentum $\mathbf{p} = -\mathbf{y}$ and averaged over all components of the nucleon momentum perpendicular to $\mathbf{q}$. It is worth mentioning that the choice of the kinematical factor K [54,55] is less relevant in nuclear matter than in finite systems, where one has extra terms due to the recoiling nucleus. In fact, in the limit $A \to \infty$, the ratio between $|\partial\omega/\partial y|$ and $|\partial\omega/\partial p_{\parallel}|_{p=p_{\min}(E_{\min})}$ is equal to $1+y/q$, which becomes 1 for large q.

In the limit $q=\infty$, and for negligible excitation energy of the final $(A-1)$ system, i.e., when the spectral function $P(\mathbf{p},E)$ may be represented by a momentum distribution $n(p)$, $F(y)$ should depend on y only, and represent the momentum distribution $n(k_{\parallel})$.

This scaling has been shown to work very well for light nuclei [56] while for heavier nuclei [10] important deviations have been observed. A recent review of both experimental observation and theoretical studies has been given by Day *et al.* [55].

The occurrence of scaling, and the approach to the $q=\infty$ limit, can give important clues on the reaction mechanism. Deviations from scaling are expected for

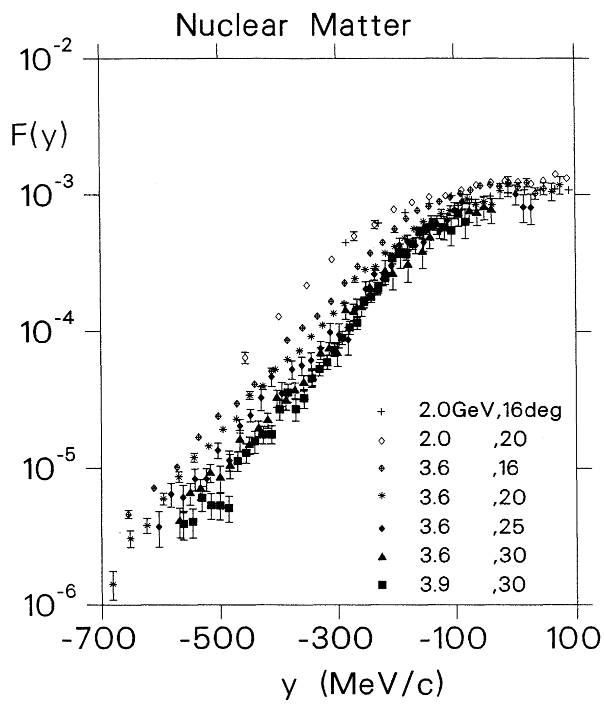

FIG. 11. Scaling function $F(y)$ for the nuclear matter data at momentum transfers q between 1 and 2 GeV/c.

two main reasons. The distribution of strength of $P(\mathbf{p},E)$ over an extended range of E leads to a convergence of $F(y)$ from below for increasing momentum transfer q. The final-state interaction of the knocked-out nucleon leads, in general, to a convergence from above. For the kinematical range of the data available for nuclear matter, it is, in particular, the latter which has a large effect. Due to the high density of nuclear matter, the effect of FSI is large.

In Fig. 11 we show the scaling function $F(y)$ for the nuclear matter data at momentum transfers between 1 and 2 GeV/c. The data corresponding to different q cover a rather broad band in $F(y)$, indicating poor scaling.

Figures 12 show the convergence of $F(y,q)$ for two selected values of y. At $y=-100$ MeV/c, a value below the Fermi momentum k_F, the quality of scaling is very good, and $F(y)$ changes little over the accessible q range. Experiment and calculation are in good agreement. The main effect of the calculated FSI in this region results from the small smearing effect of the folding [see Eq. (3.8)] from the main peak of the folding function. For $y=-500$ MeV/c $F(y,q)$ changes a factor of 3 over the accessible q range. While at low q, the rate of change is larger than the one given by the calculation, at high q the rate of convergence is close to the one calculated. In this region of y, the change of $F(y)$ with q basically results from the folding of the response due to the FSI, with the tails of the folding function moving strength from $k<k_F$ to the region $k>k_F$ where, in IA, the strength is very low. The rather good agreement of experiment and cal-

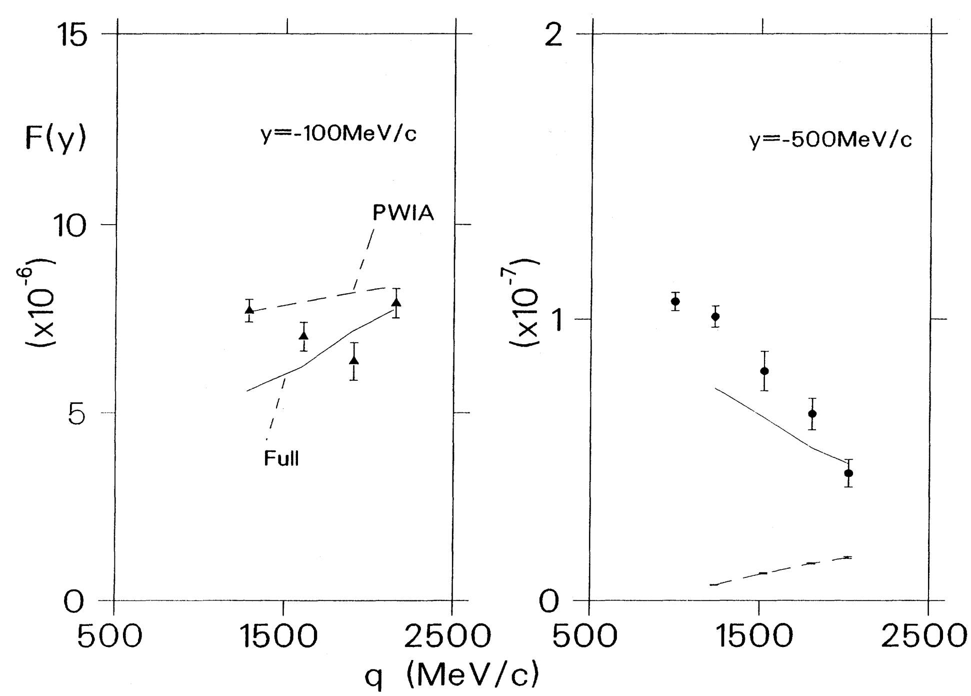

FIG. 12. Scaling functions $F(y,q)$ as a function of q for $y=-100$ and -500 GeV/c. The experimental data are compared to the PWIA estimates (dashes) and to the results of the full calculation (solid line).

culation indicates that the tails of the folding function are properly predicted. Due to the folding effect, the value of $F(y)$ at the largest q is still significantly above the PWIA value. To reach the PWIA at larger q, $F(y)$ would have to decrease another 40%.

VI. CONCLUSIONS

In this paper we have tried to quantitatively understand the response function of nuclear matter at high q. Particularly, the low-omega cross section provides fundamental information on the short-range structure of the nuclear matter wave function.

Realistic analyses of this interesting kinematical region of the nuclear matter response could not be performed in the past both for experimental and theoretical reasons. Data for nuclear matter can only be obtained by measuring the inclusive cross section for different complex nuclei and using the same kinematical conditions. Such data became available only recently [10,11]. The major theoretical difficulties consisted (i) in the microscopic evaluation of the nuclear matter response in the high-q region, where the struck nucleon and its FSI needs to be treated relativistically, and (ii) in the consistent calculation of the contribution of inelastic $e-N$ scattering, which, at high momentum transfer, is expected to be non-negligible even in the low energy loss tail.

We present a calculation of the nuclear matter inclusive cross section based on the spectral function, including the FSI, performed consistently for both the elastic and the inelastic nucleon contributions. The spectral function of nuclear matter has been calculated nonrelativistically for a realistic $N-N$ interaction by using correlated basis function theory [14]. The struck nucleon is treated relativistically and its FSI's are evaluated by generalizing the Glauber theory to the case of a relativistic nucleon propagating in the *same* nuclear medium to which it was bound before being struck by the electron. This amounts to taking into account the fact that such a nucleon, being a part of the ground state before the interaction with the electron, experiences a nucleonic density $\rho g(r)$ instead of ρ, where $g(r)$ represents the NN distribution function. It has to be noted that such a feature should never be disregarded when treating the FSI in processes where an initially bound nucleon is knocked out. In fact, it has an effect which is qualitatively similar and quantitatively much larger than that of the color transparency; the pair distribution function $g(r)$ is very small at small r and therefore the motion of the struck nucleon is little damped at distances ≤ 1 fm from where it has interacted with the electron.

The sensitivity of the cross-section to $g(r)$ is actually quite pronounced. In Fig. 13 we show the inclusive cross sections at 3.6 GeV, 25°, calculated for both the normal nuclear matter $g(r)$ and a modified $g_{\rm red}(r)$. In $g_{\rm red}(r)$ we have artificially increased by 20% the hole in $g(r)$ around $r=0$, due to short range correlations, by simply expanding the radial scale. The effect on the cross section is significant. This sensitivity to $g(r)$ is most welcome, as in most observables the effects of $N-N$ correlations are hidden and indirect. This sensitivity provides a strong motivation to study (e,e') at large q in more detail in the future.

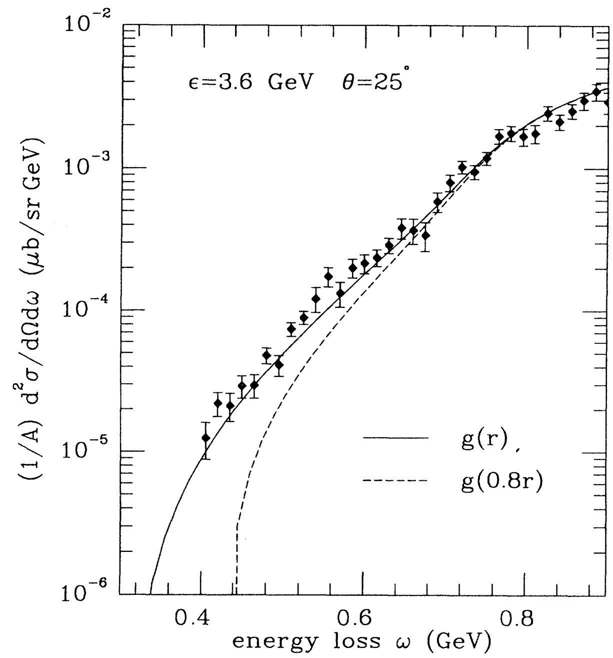

FIG. 13. Sensitivity of the inclusive cross section to the N-N pair distribution function at $\epsilon=3.6$ GeV and $\theta=25°$.

Corrections to the FSI due to color transparency are easily included in the correlated Glauber treatment. It has been found that they are indeed necessary for a better agreement with the data. Both the elastic and inelastic scattering of the electron by an off-shell nucleon has been described by using the full nuclear matter spectral function and the prescription proposed by de Forest [13] to treat the off-shell elastic e-nucleon cross section.

The results obtained show overall a good agreement with the data. For all the kinematical cases studied, the PWIA reproduces the measured cross sections near and above the top of the quasielastic peak, whereas it underestimates them at lower energy loss, where the theoretical curves lie a factor of 3–10 below the data. The main contribution to the FSI comes from the imaginary part of the optical potential. Including it by using the correlated Glauber theory plus color transparency provides a satisfactory description of the data. This implies, on one side, that both the spectral function and the treatment of the nucleon inelastic contributions used in this work are quite realistic and, on the other side, that FSI's are quite large at low ω.

We note that the present calculations involve two main approximations: (i) the use of de Forest's method to estimate the off-shell electron-nucleon cross sections, and (ii) the use of the first-order-correlated Glauber approximation to estimate the FSI effects. Both these approximations appear to be reasonable, but it is desirable to ascertain their accuracy quantitatively. Data at higher values of q and ω will also be helpful in studying color transparency. Exclusive $(e,e'p)$ measurements in the region of the quasifree peak [57] may also provide further evidence of this effect.

The FSI bring the PWIA results close to the data, however, at very-low-energy loss $\omega < 0.5$ GeV there are substantial differences between the calculated and observed response. Part of the discrepancies, particularly visible at $\epsilon = 3.595$ GeV, $\theta = 20°$ are due to the fact that the momentum and the energy of the struck nucleon are not strictly those of the quasifree kinematics, as considered here, but rather they depend upon the initial-state of the nucleon. Moreover, it is likely that the first-order-correlated Glauber approximation used in the treatment of the FSI is less valid at lower values of the recoil-nucleon momentum. It will be necessary to go beyond the first-order approximation in the $q \sim 3-7$ fm^{-1} and $\omega < 0.5$ GeV region where the purely nonrelativistic theory [20] is not applicable, and where the present approach also seems not to be adequate.

ACKNOWLEDGMENTS

The authors wish to thank Luciano Bertocchi, Alex Dieperink, and Daniele Treleani for illuminating discussions and Herman Grunder and Dirk Walecka for their kind hospitality at CEBAF. This work was partly supported by Istituto Nazionale di Fisica Nucleare, U.S. National Science Foundation via Grant No. PHY 89-21025, US-DOE, and the Swiss National Science Foundation.

[1] H. Bethe, Annu. Rev. Nucl. Sci. **21**, 93 (1971).
[2] A. Bohr and B. Mottelson, *Nuclear Structure* (Benjamin, New York, 1969), Vol. I.
[3] *Proceedings of Cargese Summer School France, 1989,* edited by V. R. Pandharipande, J. Tran Thanh Van, and J. W. Negele (Plenum, New York, 1990).
[4] J. M. Cavedon *et al.*, Phys. Rev. Lett. **49**, 978 (1982).
[5] P. Barreau *et al.*, Nucl. Phys. **A402**, 515 (1983).
[6] C. C. Blatchley *et al.*, Phys. Rev. C **34**, 1243 (1986).
[7] Z. E. Meziani *et al.*, Phys. Rev. Lett. **52**, 2130 (1984).
[8] M. Deady *et al.*, Phys. Rev. C **33**, 1897 (1986).
[9] D. B. Day, J. S. McCarthy, I. Sick, R. G. Arnold, B. T. Chertok, S. Rock, Z. M. Zsalata, F. Martin, B. A. Mecking, and G. Tamas, Phys. Rev. Lett. **43**, 1143 (1979).
[10] D. B. Day *et al.*, Phys. Rev. Lett. **59**, 427 (1987).
[11] D. B. Day *et al.*, Phys. Rev. C **40**, 1011 (1989).
[12] T. de Forest, Jr., Nucl. Phys. **A392** 232 (1983).
[13] C. Itzykson and J. B. Zuber, *Quantum Field Theory* (McGraw-Hill, New York, 1980).
[14] O. Benhar, A. Fabrocini, and S. Fantoni, Nucl. Phys. **A505**, 267 (1989).
[15] S. Frullani and J. Mougey, Adv. Nucl. Phys. **14**, 1 (1984).
[16] P.K.A. De Witt Huberts, J. Phys. G **16**, 507 (1990).
[17] M. N. Butler and S. E. Koonin, Phys. Lett. B **205**, 123 (1988).
[18] A.E.L. Dieperink, T. de Forest, Jr., I. Sick, and R. A. Brandenburg, Phys. Lett. **63B**, 261 (1976).
[19] A. Bodek and J. L. Ritchie, Phys. Rev. D **23**, 1070 (1981).
[20] S. Fantoni and V. R. Pandharipande, Nucl. Phys. **A473**, 234 (1987).
[21] A. Fabrocini and S. Fantoni, Nucl. Phys. **A503**, 375 (1989).
[22] E. Manousakis and V. R. Pandharipande, Phys. Rev. B **33**, 150 (1986).
[23] A. Belic and V. R. Pandharipande, Phys. Rev. B (to be published).
[24] Y. Horikawa, F. Lenz, and N. C. Mukhopadhyay, Phys. Rev. C **22**, 1680 (1980).
[25] L. J. Rodriguez, H. A. Gersch, and H. A. Mook, Phys. Rev. A **9**, 2085 (1974).
[26] P. M. Platzman and N. Tzoar, Phys. Rev. B **30**, 6397 (1984).
[27] R. Silver and G. Reiter, Phys. Rev. B **35**, 3647 (1987).
[28] R. Silver, Phys. Rev. B **38**, 2283 (1988).
[29] E. D. Cooper, B. C. Clark, S. Hama, and R. L. Mercer, Phys. Lett. B **206**, 588 (1988).
[30] B. C. Clark, private communication.
[31] R. Schiavilla, D. S. Lewart, V. R. Pandharipande, S. C. Pieper, R. B. Wiringa, and S. Fantoni, Nucl. Phys. A **473**, 267 (1987).
[32] R. J. Glauber, in *Lectures in Theoretical Physics,* edited by W. E. Brittin *et al.* (Interscience Publishers, Inc., New York, 1959).
[33] D. F. Jackson, *Nuclear Reactions* (Methuen, London, 1970).
[34] R. H. Bassel and C. Wilkin, Phys. Rev. Lett. **18**, 871 (1967).
[35] A. V. Dobrovolsky *et al.*, Nucl. Phys. B **214**, 1 (1983).
[36] B. H. Silverman *et al.*, Nucl. Phys. **A499**, 763 (1989).
[37] T. Uchiyama, A.E.L. Dieperink, and O. Scholten, Phys. Lett. B **233**, 31 (1989).
[38] R. Schiavilla, V. R. Pandharipande, and R. B. Wiringa, Nucl. Phys. **A449**, 219 (1986).
[39] S. J. Brodsky, in *Proceedings of the XIII International Symposium on Multiparticle Dynamics,* Volendam, The Netherlands, 1982, edited by W. Metzgen, E. W. Kittel, and A. Stergion (World-Scientific, Singapore, 1982).
[40] A. Mueller, in *Proceedings of the XVI Rencontre de Moriond, Les Arcs, France, 1982,* edited by J. Tran Thanh Van (Editions Frontieres, Gif-sur-Yvette, 1982).
[41] G. R. Farrar, H. Liu, L. L. Frankfurt, and M. E. Strickman, Phys. Rev. Lett. **61**, 686 (1988).
[42] B. K. Jennings and G. A. Miller, Phys. Lett. B **237**, 209 (1990); Phys. Rev. D **44**, 692 (1991).
[43] L. L. Frankfurt and M. I. Strickman, Phys. Rep. **160**, 235 (1987).
[44] I. E. Lagaris and V. R. Pandharipande, Nucl. Phys. **A359**, 331 (1981).
[45] I. E. Lagaris and V. R. Pandharipande, Nucl. Phys. **A359**, 349 (1981).
[46] A. Fabrocini and S. Fantoni, in *First Course on Condensed Matter,* edited by D. Prosperi, S. Rosati, and G. Violini (World-Scientific, Singapore, 1986), Vol. VIII, pp. 87–153.
[47] S. Fantoni and V. R. Pandharipande, Phys. Rev. C **37**, 1697 (1988).
[48] S. Fantoni, B. L. Friman, and V. R. Pandharipande, Nucl. Phys. **A399**, 51 (1983).
[49] E. D. Cooper, B. C. Clark, R. Kozack, S. Shim, S. Hama,

J. I. Johanson, H. S. Sherif, R. L. Mercer, and B. D. Serot, Phys. Rev. C **36**, 2170 (1987).
[50] P. Schwandt, in *The Interactions Between Medium Energy Nucleons in Nuclei (Indiana Cyclotron Facility, Bloomington, Indiana),* Proceedings of the Workshop on the Interactions Between Medium Energy Nucleons in Nuclei, AIP Conf. Proc. No. 97, edited by Hans-Otto Meyer (AIP, New York, 1983), p. 29.
[51] D. Frekers *et al.*, Phys. Rev. C **35**, 2236 (1987).
[52] G. Höhler, E. Pietarinen, I. Sabba-Stefanescu, F. Borkowski, G. G. Simon, V. H. Walther, and R. D. Wendling, Nucl. Phys. **B114**, 505 (1976).
[53] E. Pace and G.Salme', Phys. Lett. **110B**, 411 (1982).
[54] C. Ciofi degli Atti, E. Pace, and G. Salme', Phys. Lett. **127B**, 303 (1983).
[55] D. B. Day, J. S. McCarthy, T. W. Donnelly, and I. Sick, Annu. Rev. Nucl. Part. Sci. **40**, 357 (1990).
[56] I. Sick, D. Day, and J. S. McCarthy, Phys. Rev. Lett. **45**, 871 (1980).
[57] J. Van den Brand *et al.*, SLAC-NPAS Report NE18, 1990.